

## PAPER

[View Article Online](#)  
[View Journal](#) | [View Issue](#)Cite this: *RSC Adv.*, 2019, 9, 37144Received 23rd July 2019  
Accepted 29th October 2019

DOI: 10.1039/c9ra05709a

[rsc.li/rsc-advances](http://rsc.li/rsc-advances)

# Visual detection of *Fusarium proliferatum* based on asymmetric recombinase polymerase amplification and hemin/G-quadruplex DNAzyme†

Ying Wang,<sup>a</sup> Xiangdong Li,<sup>b</sup> Dongmei Xi<sup>a</sup> and Xiaoqiang Wang<sup>c</sup>

A one-step and instrument-free visual method was established based on asymmetric recombinase polymerase amplification coupled with hemin/G-quadruplex DNAzyme for the detection of *Fusarium proliferatum*.

*Fusarium proliferatum* causes rot disease, which is difficult to control worldwide. The vascular systems of *F. proliferatum*-infected crops are destroyed. It causes rot of the stems, stalks, roots, flowers, and ears of maize<sup>1–3</sup> and decreases its yield and quality remarkably. In addition, the mycotoxins of fumonisin B1, fumonisin B2, beauvericin, enniatins, fusaproliferin, and moniliformin are produced by *F. proliferatum* during infection processes.<sup>4–6</sup> When these grains are used as food or feedstuffs, the health of consumers or livestock is exposed to danger.<sup>7</sup> There are many reports on the illnesses of livestock and humans caused by *Fusarium* mycotoxins.<sup>8–10</sup> Methods based on qPCR have been developed for *F. proliferatum* detection.<sup>11</sup> Although they show high accuracy, these methods require expensive instruments and skilled operators; they are also limited by many factors, such as electric power, high cost, and long testing times, which results in inability to apply these methods outside the lab. Therefore, sensitive and simple detection of *F. proliferatum* is still needed in field testing of crops and their byproducts.

Bio-sensing has become important in recent decades because it provides alternative methods to solve some of the above problems.<sup>12–14</sup> Recombinase polymerase amplification (RPA)<sup>15</sup> is a conventional and isothermal method to obtain double-stranded DNA (dsDNA). There are many reports of rapid detection based on RPA,<sup>16</sup> such as monitoring of viruses, plasmodium, mycoplasma, fungi, and other causative agents. End-point detection is usually performed using lateral flow strips.<sup>17–19</sup> The greatest strengths of the lateral flow strip method

are that it is rapid and straightforward. However, its cost is quite high because of the primer labeling and preparing of the strips. In addition, the strip is disposable, which is not suitable for high throughput detection. The product of RPA can also be observed with the aid of SYBR Green I in UV light.<sup>20</sup> However, there is no selectivity of binding between SYBR Green I and dsDNA, which results in false positive results of primer dimers and nonspecific amplification of other dsDNA.

Methods of visual detection are greatly valued due to the intuitiveness of the results.<sup>21</sup> Gold nanoparticles are widely used for colorimetric detection of various targets.<sup>22</sup> However, preparation of gold nanoparticles with specific sizes is laborious and difficult. Proteins, genomic DNA, salts, *et al.* are present in the crude liquids of biological samples used in point-of-care detection, which may give rise to nonspecific aggregation of gold nanoparticles. Hemin/G-quadruplex-based visual methods are used to detect targets of nucleotides, proteins, and other signal molecules.<sup>23</sup> In the presence of hemin/G-quadruplex DNAzyme, H<sub>2</sub>O<sub>2</sub> and ABTS<sup>2–</sup> react, and a specific green color is observed; this method is very simple, cost-effective, and straightforward compared with lateral flow strips or gold nanoparticles.

Asymmetric RPA is a type of amplification that involves different concentration ratios of primer-F/primer-R. First, the dsDNA product is obtained with the primer pair. As the reaction continues, one primer in a small amount is exhausted, and single-stranded DNA (ssDNA) is produced by the other primer using the newly synthesized dsDNA as a template. In this paper, an one-step and instrument-free strategy for visual monitoring of *F. proliferatum* is established based on asymmetric recombinase polymerase amplification coupled with hemin/G-quadruplex DNAzyme.

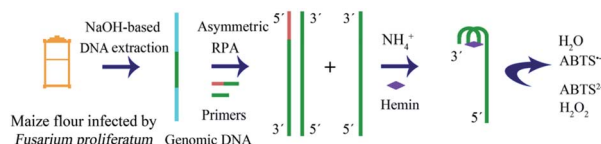
The strategy is shown in Scheme 1; it includes extraction of genomic DNA of *F. proliferatum* DSM62267 (F120), asymmetric RPA, and visual detection. First, genomic DNA was released from F120 cells with NaOH solution. It was used directly as a template for asymmetric RPA with primer-F and primer-R in

<sup>a</sup>College of Life Science, Shandong Provincial Key Laboratory of Detection Technology for Tumor Markers, School of Chemistry and Chemical Engineering, Linyi University, Linyi 276005, People's Republic of China. E-mail: wangying@lyu.edu.cn

<sup>b</sup>Shandong Province Key Laboratory of Agricultural Microbiology, College of Plant Protection, Shandong Agricultural University, Tai'an, Shandong 271018, People's Republic of China

<sup>c</sup>Plant Protection Research Center, Tobacco Research Institute of Chinese Academy of Agricultural Sciences, Qingdao 266101, People's Republic of China

† Electronic supplementary information (ESI) available. See DOI: 10.1039/c9ra05709a



**Scheme 1** Schematic of the asymmetric recombinase polymerase amplification and hemin/G-quadruplex DNAzyme-based visual detection of *F. proliferatum*.

a certain ratio. The *trans*-complementary sequence of the G-quadruplex was designed at the 5'-terminal of primer-F. The RPA product was obtained in the presence of a TwistDx/Twist-Amp® Liquid Basic kit. The product was a mixture of dsDNA and ssDNA with the G-quadruplex sequence at their 3'-ends. In the presence of  $\text{NH}_4^+$  and hemin, a DNAzyme of hemin/G-quadruplex was constructed at the end of the ssDNA. When  $\text{ABTS}^{2-}$  and  $\text{H}_2\text{O}_2$  were added, the resulting solution turned green. However, no color changes occurred in the final solution if no F120 genomic DNA was present, no target DNA was extracted, or no ssDNA was amplified by asymmetric RPA.

A genomic DNA mixture of maize and F120 was extracted from maize flour using NaOH solution. The feasibility of the asymmetric RPA reaction<sup>24</sup> was evaluated using this genomic DNA as a template. The ratios of primer-F and primer-R were set as 1 : 1, 1 : 10, 1 : 20, 1 : 50, 1 : 75, and 1 : 100. The products were analyzed by 2.5% agarose gel electrophoresis and stained with ethidium bromide. As shown in Fig. 1A, the bands of ssDNA were all in front of the bands of dsDNA, compared with the band of the 1 : 1 ratio of the primer pair (1). Faint bands of ssDNA were observed when the ratio of primer-F and primer-R was 1 : 75 (5) or 1 : 100 (6). When the ratio was 1 : 20 (3), the band of ssDNA was brighter than those of 1 : 10 (2) and 1 : 50 (4). The yellow line represents the leading edge of the ssDNA bands. At the same time, the bands of dsDNA tapered off with the appearance of ssDNA and the down-ratio of primer-F/primer-R. These data show that genomic DNA of F120 could be extracted by NaOH solution, and the unpurified template of F120 was available for asymmetric RPA. In

addition, more ssDNA was produced by the primer pair ratio of 1 : 20 than the other ratios; thus, this ratio was used in the following tests.

To demonstrate the feasibility of the asymmetric RPA-hemin/G-quadruplex assay, the absorbance of the resulting solutions was measured by UV-Vis absorption (390 to 490 nm) of NanoDrop 2000. As shown in Fig. 1B, no absorption signal was observed in solutions containing hemin,  $\text{H}_2\text{O}_2$  and  $\text{ABTS}^{2-}$  (a) or the assay without genomic F120 DNA near 420 nm (b). An obvious increase of absorbance was observed in the presence of the target DNA (c) at 420 nm. A specific green color appeared in tube c (inserted in the top right corner of Fig. 1B). This result was in keeping with that of the UV-Vis absorption, demonstrating that the asymmetric RPA coupled with hemin/G-quadruplex DNAzyme method is viable. The visual biosensor could monitor *F. proliferatum* in maize flour.

The intensity of UV-Vis absorption generated by the asymmetric RPA-hemin/G-quadruplex assay depended on the temperature gradient and time of the RPA reaction, as well as the different monovalent cations in the final solution (Fig. S1–S3†). To assess the analytical performance of the asymmetric RPA-hemin/G-quadruplex assay, various amounts of F120 genomic DNA were monitored under the optimal conditions. The UV-Vis absorption increased with the amount of F120 DNA from 0 to 50 ng (Fig. 2A). A larger amount of F120 DNA was used as the template, and more ssDNA was produced by the asymmetric RPA reaction. More hemin/G-quadruplex DNAzyme was constructed, causing an increase of the UV-Vis absorption of the resulting solution. A good linear dependence was observed between the absorbance and the amount of genomic DNA of F120 in a range from 0.01 ng to 50 ng at 420 nm (Fig. 2B and S4†). The regression equation was  $A = 0.1042 \lg m + 1.331$ , with a correlation coefficient of 0.989, in which  $A$  and  $m$  represent the absorbance and quantity of F120 genomic DNA. The detection limit was calculated to be 0.01 ng by three times the standard deviation of the blank. The type of reaction vessel, reaction temperature, and sensitivity of the proposed strategy were compared with RPA-related colorimetric detection methods (ESI Table 1†).

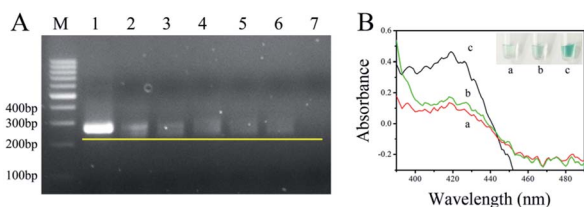


**Fig. 1** (A) 2.5% agarose gel electrophoresis analysis of asymmetric RPA with ratios of primer-F/primer-R of 1 : 1 (1), 1 : 10 (2), 1 : 20 (3), 1 : 50 (4), 1 : 75 (5), and 1 : 100 (6). Line 7 is the blank control, and genomic DNA of healthy maize flour was used as the template. The yellow line represents the leading edge of the ssDNA bands. (B) Colorimetric detection of the solution (pH 7.9) containing 0.6  $\mu\text{M}$  hemin, 150 mM  $\text{NH}_4\text{Cl}$ , 2 mM  $\text{H}_2\text{O}_2$ , and 2 mM  $\text{ABTS}^{2-}$  within the wavelength range of 390 to 490 nm, (a) blank control, (b) in the absence and (c) in the presence of genomic DNA of *F. proliferatum* at the primer-F/primer-R ratio of 1 : 20. The inset in B is an image of the resulting colors with the corresponding samples.

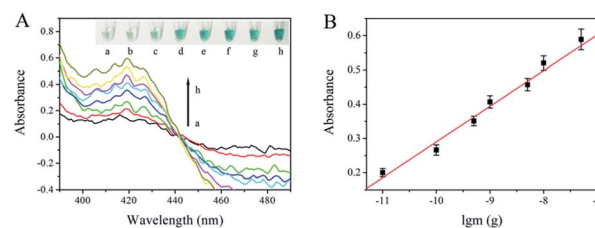


**Fig. 2** (A) Absorption curves of solutions containing various amounts of genomic DNA of F120 in the wavelength range of 390 to 490 nm. The arrow from a to h represents DNA amounts of 0 ng (a), 0.01 ng (b), 0.1 ng (c), 0.5 ng (d), 1 ng (e), 5 ng (f), 10 ng (g), and 50 ng (h). The inset shows an image of the visual detection of the corresponding quantities of genomic F120 DNA. (B) The linear correlation between the absorbance and the negative logarithm of genomic F120 DNA quantity at 420 nm.



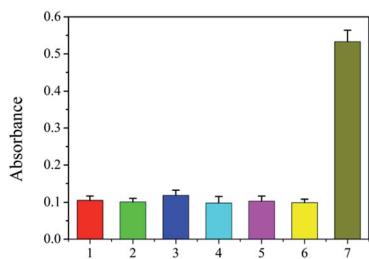


Fig. 3 Selectivity of the proposed method. (1) Blank control, (2) *F. equiseti* RD13, (3) *F. culmorum* 3.37 dus Bomm, (4) *F. avenaceum* borm, (5) *R. solanacearum*, (6) *P. sorghi*, and (7) *F. proliferatum* DSM62267.

The selectivity of the proposed assay is critical because numerous DNA sequences belonging to the host and other living bodies are present in biological samples. The primer pair used in the strategy was based on the intergenic sequence of the ribosomal RNA gene cluster, which is specific to species of *F. proliferatum*. Three fungi, *F. equiseti* RD13 (F216), *F. culmorum* 3.37 dus Bomm (F109), and *F. avenaceum* borm (F112), are also species of *Fusarium*. *Ralstonia solanacearum* and *Puccinia sorghi* are common causes of disease in corn. The three *Fusarium* species, *R. solanacearum*, and *P. sorghi* were used as controls to check the selectivity of the proposed strategy. As shown in Fig. 3, the absorbances of the final solutions of *F. equiseti* RD13 (2), *F. culmorum* 3.37 dus Bomm (3), *F. avenaceum* borm (4), *R. solanacearum* (5), and *P. sorghi* (6) were as low as that of the blank control (1). However, the absorbance from genomic F120 DNA (7) was obviously high, showing the good selectivity of our strategy.

To demonstrate the feasibility of the proposed assay for real sample detection, 4 positive samples and 10 field-collected samples were successively tested by the RPA/G-quadruplex visual assay and PCR. The results show that 2 of the 8 field-collected samples were infected with *F. proliferatum*; also, the two methods were consistent, indicating that our RPA/G-quadruplex visual strategy is plausible and can be used in field tests (Table 1).

This strategy has obvious advantages. It employs specific primers of *F. proliferatum*, guaranteeing good sensitivity and selectivity of the biosensor over other species of *Fusarium*. Asymmetric RPA and hemin/G-quadruplex strategies were combined to achieve visual detection of *F. proliferatum*; the method is very simple, straightforward and cost-effective. The strategy is instrument-free, and only two label-free oligonucleotides were used in the assay, which was performed in a foam

box with hot water; this implies that the proposed assay can be applied in field tests.

Therefore, the one-step and instrument-free visual detection of *F. proliferatum* species based on asymmetric RPA coupled with hemin/G quadruplex DNAzyme was established. The asymmetric RPA reaction was performed in a foam box with hot water, and the results of a specific green color could be observed by the naked eye. The method is label-free and extremely simple, and it can be operated by general staff; thus, it has great potential for field tests. The proposed strategy has good sensitivity, with a detection limit of 0.01 ng by absorption spectroscopy. It shows satisfactory selectivity for *F. proliferatum* species over other *Fusarium* species. It also has great potential to be applied to detect other DNA-based samples, such as viruses, bacteria, fungi, plants and animals, by changing the corresponding specific primers.

## Conflicts of interest

There are no conflicts to declare.

## Acknowledgements

The authors would like to acknowledge the assistance of Professor Petr Karlovsky from the University of Goettingen, Germany, for kindly providing strains of *F. proliferatum* DSM62267, *F. equiseti* RD13, *F. culmorum* 3.37 dus Bomm, *F. avenaceum* borman, and maize flour contaminated with *F. proliferatum* DSM62267. This work was financially supported by the National Natural Science Foundation of China (No. 31701760, 31901937), Shandong Provincial Major Application Technology Innovation Project, and Shandong Provincial National Science Foundation (ZR2018BC037).

## Notes and references

- 1 A. Logrieco, A. Rizzo, R. Ferracane and A. Ritieni, *Appl. Environ. Microbiol.*, 2002, **68**, 82–85.
- 2 J. H. Choi, S. Lee, J. Y. Nah, H. K. Kim, J. S. Paek, S. Lee, H. Ham, S. K. Hong, S. H. Yun and T. Lee, *Int. J. Food Microbiol.*, 2018, **267**, 62–69.
- 3 E. Cendoya, M. D. P. Monge, S. M. Chiacchiera, M. C. Farnochi and M. L. Ramirez, *Int. J. Food Microbiol.*, 2018, **266**, 158–166.
- 4 L. Morales, T. P. Marino, A. J. Wenndt, J. Q. Fouts, J. B. Holland and R. J. Nelson, *Phytopathology*, 2018, **108**, 1475–1485.
- 5 Q. Jian, T. Li, Y. Wang, Y. Zhang, Z. Zhao, X. Zhang, L. Gong and Y. Jiang, *Food Res. Int.*, 2019, **116**, 397–407.
- 6 M. Bryla, A. Waskiewicz, E. Ksieniewicz-Wozniak, K. Szymczyk and R. Jedrzejczak, *Molecules*, 2018, **23**, 963–996.
- 7 S. Yazar and G. Z. Omurtag, *Int. J. Mol. Sci.*, 2008, **9**, 2062–2090.
- 8 I. Zimmer, E. Usleber, H. Klaffke, R. Weber, P. Majerus, H. Otteneder, M. Gareis, R. Dietrich and E. Martlbauer, *Mycotoxin Res.*, 2008, **24**, 40–52.

Table 1 Field monitoring based on RPA/G-quadruplex visual assay

Sample	PCR-based detection		RPA/G-quadruple-based detection	
	Positive	Negative	Positive	Negative
4	4	0	4	0
10	2	8	2	8



- 9 H. K. Abbas, W. P. Williams, G. L. Windham, H. C. Pringle 3rd, W. Xie and W. T. Shier, *J. Agric. Food Chem.*, 2002, **50**, 5246–5254.
- 10 H. F. Vismer, G. S. Shephard, J. P. Rheeder, L. van der Westhuizen and R. Bandyopadhyay, *Food Addit. Contam., Part A: Chem., Anal., Control, Exposure Risk Assess.*, 2015, **32**, 1952–1958.
- 11 S. Nutz, K. Doll and P. Karlovsky, *Anal. Bioanal. Chem.*, 2011, **401**, 717–726.
- 12 Y. Wang, B. X. Li, J. Liu and H. Zhou, *Sens. Actuators, B*, 2018, **273**, 649–655.
- 13 Y. Wang, B. Li, J. Liu and H. Zhou, *Anal. Bioanal. Chem.*, 2019, 2915–2924.
- 14 D. Xi, X. Wang, S. Ai and S. Zhang, *Chem. Commun.*, 2014, **50**, 9547–9549.
- 15 S. Lutz, P. Weber, M. Focke, B. Faltin, J. Hoffmann, C. Muller, D. Mark, G. Roth, P. Munday, N. Armes, O. Piepenburg, R. Zengerle and F. von Stetten, *Lab-on-a-Chip*, 2010, **10**, 887–893.
- 16 J. Li, J. Macdonald and F. von Stetten, *Analyst*, 2019, **144**, 31–67.
- 17 S. H. Kim, J. Lee, B. H. Lee, C. S. Song and M. B. Gu, *Biosens. Bioelectron.*, 2019, **134**, 123–129.
- 18 X. Deng, C. Wang, Y. Gao, J. Li, W. Wen, X. Zhang and S. Wang, *Biosens. Bioelectron.*, 2018, **105**, 211–217.
- 19 M. L. Powell, F. R. Bowler, A. J. Martinez, C. J. Greenwood, N. Armes and O. Piepenburg, *Anal. Biochem.*, 2018, **543**, 108–115.
- 20 R. Wang, F. Zhang, L. Wang, W. J. Qian, C. Qian, J. Wu and Y. B. Ying, *Anal. Chem.*, 2017, **89**, 4413–4418.
- 21 Y. Wang, J. Liu and H. Zhou, *Sensors*, 2019, **19**, 1298.
- 22 E. Priyadarshini and N. Pradhan, *Sens. Actuators, B*, 2017, **238**, 888–902.
- 23 Z. Tang, H. Zhang, C. Ma, P. Gu, G. Zhang, K. Wu, M. Chen and K. Wang, *Microchim. Acta*, 2018, **185**, 109.
- 24 U. B. Gyllensten and H. A. Erlich, *Proc. Natl. Acad. Sci. U. S. A.*, 1988, **85**, 7652–7656.

